9.4 CALIBRATION OF THE VIIRS DAY/NIGHT BAND (DNB)

Steve Mills*[a], Eric Jacobson[b], Jackie Jaron[†c], James McCarthy[a],
Tohru Ohnuki [a], Mike Plonski [a], Don Searcy[a], Stephanie Weiss[a]
[a]Northrop Grumman Aerospace Systems (NGAS), Redondo Beach, California
[b]Raytheon Company, El Segundo, California
[c]Millennium Space Systems

1. INTRODUCTION

The Day/Night Band (DNB) on the Visible Infrared Imager Radiometer Suite (VIIRS) is part of the National Polar-orbiting Operational Environmental Satellite System (NPOESS) and the NPOESS Preparatory Program (NPP). NPOESS is the U.S. next generation weather and climate monitoring system administered by DoD, DoC, and NASA.

The DNB is a panchromatic solar reflective band with a dynamic range capable of detecting Earth scenes as dim as quarter moon illumination to the brightest daytime—over 7 orders of magnitude in dynamic range. To achieve this large dynamic range it uses a 3 stage focal plane.

The sensor maintains a nearly constant 0.75 km resolution over the entire 3000 km swath using an on-board aggregation scheme. This fact, combined with the 3 gain stages makes on-orbit calibration of the DNB a complex process. This paper describes the on-orbit calibration process in detail.

2. MISSION OF DNB

The DNB has a primary and a secondary mission that it inherits from its heritage instrument, the Operational Linescan System (OLS) on the Defense Meteorological Satellite Program (DMSP) satellite.

2.1 *Primary Mission*

The primary mission of the DNB is defined in the NPOESS requirements. It is to produce imagery of clouds continuously for the day, night and twilight (near terminator) scenes observed by VIIRS (Hutchison 2005). The DNB is required to maintain a resolution of about 750 m over the entire 3000 km wide swath. Because of the 3000 km swath width and the NPOESS/NPP orbit it is able to provide global coverage with 12 hour revisit time for cloud imagery under solar and lunar illumination down to quarter moon (Miller 2005).

It should be noted that this primary mission does not actually require radiometric calibration, and in fact the heritage sensor, OLS, does not perform any radiometric calibration. Rather, since the mission is to produce imagery that is uniform (e.g. no striping) that can easily be interpreted by an image analyst, it only requires good relative radiometry, and so absolute radiometric calibration is not the goal (Lee 2006).

2.2 *Secondary Mission*

Though the OLS was originally designed specifically for the primary mission of cloud imagery, the declassification of its data in the 1970's and its sensitivity to low radiance levels created interest by researchers in a number of areas that were not part of the original OLS mission. This includes observations of aerosols at night such as dust storms and smoke (Lee 2006); the aurora (Akasofu 1974); fire detection at night (Elvidge 1996; Elvidge 1998); lightning at night (Orville 1981; Orville 1986); nighttime snow (Foster 1983; Foster 1991); bioluminescence (Miller 2006); and man-made light sources (Elvidge 1997). Man-made light sources include electric lights on land or from ships, gas flares and campfires.

All of these discovered uses for OLS data have given OLS many secondary missions and the DNB will inherit these missions. Unfortunately the OLS design did not anticipate these, which all require radiometric calibration. Therefore it is necessary to operate OLS in special modes

*Corresponding author address: Steve Mills, Northrop Grumman Aerospace Systems, One Space Park, Redondo Beach, CA 90278; e-mail stephen.mills@ngc.com

† J. Jaron contributed to this paper while working at Northrop Grumman Aerospace Systems.

to support radiometric calibration. Fortunately, the DNB was designed to use the on-board solar diffuser calibration and its radiometric response was accurately characterized in ground testing (Jacobson 2010).

Just as OLS opened new areas of research not anticipated during its design, a well calibrated DNB could provide opportunities that were not possible with OLS. For example, it may be possible to make rough estimates of cloud optical thickness (COT) at night over urban areas using the upwelling of radiance (or lack of it) from city lights. Normally COT is determined by scattered light from the sun or moon. With city lights, a one-way transmittance could be determined by comparison to known clear sky radiances from the city, assuming the city lights are relatively constant. Of course the light passing through clouds will spread the radiance patterns (Croft 1978), and this complicates the COT estimate but it could give further clues about cloud height if properly understood.

Another area of research that could open up with the availability of the DNB is a better understanding of scattering in the terminator region – "the twilight's last gleaming". In the OLS era there has been a large amount of effort involving nighttime scenes but very little regarding the terminator or twilight region. In fact, with proper calibration of the DNB-MGS this will be the first time well calibrated Vis/NIR radiances have been measured by an operational satellite for scenes in the region around the terminator. Most radiative transfer models break down in this region and must rely on empirical measurements. The DNB data could be used to improve radiative transfer models and to gain a better understanding of atmospheric scatter.

Both ground calibration and on-orbit calibration are critical to producing well calibrated radiances, and thus to the success of these DNB secondary missions. The focus of this paper is on the on-orbit processes.

3. DNB DESCRIPTION

Table 1 below summarizes the parameters of the DNB compared with the other VIIRS reflective bands. The DNB is part of VIIRS, which was designed, built and tested by Raytheon Company. It is a panchromatic solar reflective band with a huge dynamic range capable of detecting Earth scenes as dim as quarter moon illumination to the brightest daytime solar illumination. It is sometimes even capable of detecting electric lights from a single home or boat.

Table 1 - VIIRS DNB parameters compared with other VIIRS bands

Feature	Other VIIRS Reflective Bands	Day/Night Band
Dynamic range ratio	$L_{max} / L_{min} <$ 270	L_{max} / L_{min} =6,700,000
Time Delay Integration	none	HGS=250; MGS =3; LGS=1
Aggregation	In-scan only; 3 symmetric aggregation zones	Both in-track and in-scan; 32 symmetric aggregation zones
Spatial Resolution	Imagery: 400 to 800 m; Moderate: 750 -1600 m	750 m across full scan, both directions
Cal view Samples	Imagery: 96; Moderate: 48	16 per stage;
Cal view aggregate	unaggregated	aggregated
Cal views cycles	One gain state per scan; 4 scan cycle	All gain stages per scan; 72 scan cycle
Solar cal view	About 32 scans per orbit, both gain states	MGS and HGS saturates, only LGS is useful
SDSM	8 bands: 410 to 900 nm	weighted average of 8

The DNB is able to achieve over 7 orders of magnitude in dynamic range at nadir and 6 orders at edge of scan. It achieves this by using a 3 stage focal plane, where each stage essentially functions as a separate imager though they all reside on the same CCD array. The array has much higher resolution than what is required to achieve 750 m resolution requirement, but data is combined electronically on-board through an on-chip aggregation process that varies over the scan swath.

The low-gain stage (LGS) is used to observe daytime scenes, and requires a neutral density filter to prevent saturation in full daylight. It does not employ any TDI. The mid-gain stage (MGS) is used to observe dawn or dusk scenes near the Earth's terminator, and has TDI to increase signal. The high-gain stage (HGS) is used to observe nighttime scenes with lunar illumination or late twilight and uses TDI over hundreds of pixels to maximize the signal. The HGS is actually the average of two identical stages: High Gain A (HGA) and High Gain B (HGB), and this makes it possible to filter out high energy particle strikes.

Where the DNB is distinguished most from the other VIIRS bands is with its dynamic range and its unique 3-stage design. Because of these differences the calibration process for the DNB is very different from the other reflective bands.

4. MODELING OF SCENES

In order to design and test a workable on-orbit calibration process for the DNB, it is necessary to have test scenes that approximate the earth radiances observed in day, night or around the terminator. The EVEREST simulation (Shoucri 2009; Mills 2004), developed by NGAS, was used for this purpose.

4.1 *Simulating Scene Radiance*

Because of the large amount of scattering around the terminator, modeling earth reflectance is inherently difficult. Several models within EVEREST were considered. Synthetic Data is derived from a combination of radiative transfer models (RTM) including MODTRAN. An empirical model based on MODIS proxy data from the reflective band statistics is also available.

Since MODIS reflective bands turn off for night time scenes, there is no data beyond solar zenith angle (SZA) = 93º. Comparing the MODIS proxy data statistically with the synthetic RTM data, they agree quite well for SZA from 0º to 93º (terminator is at SZA= 90º). To simulate nighttime and twilight scenes from MODIS proxy data, several MODIS bands are combined with a weighted average to simulate the panchromatic DNB. In nighttime and twilight scenes where MODIS scenes are not available, the MODIS scenes are scaled by the ratio of the solar or lunar irradiance expected over the irradiance of the daytime MODIS scene. This produces reasonably realistic simulated DNB scenes, although the surface conditions do not in any way correspond to the actual scene being simulated. The statistical distribution of the MODIS proxy data and the synthetic data are shown in Figure 1.

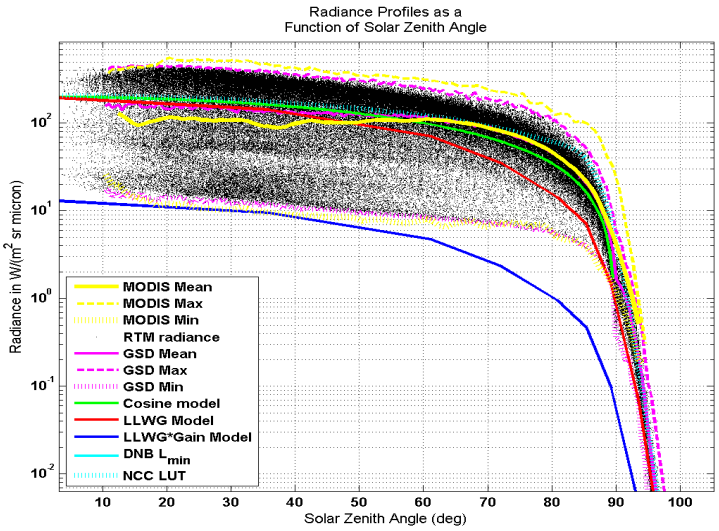

Figure 1 - Radiance vs. Solar Zenith Angle for MODIS Proxy Model and RTM Synthetic Data. LLWG model is shown for comparison.

The Low Light Working Group (LLWG) model was developed at Raytheon in the early phases of the DNB design in order to estimate where the DNB would be in each of the 3 gain stages. While it was sufficient for

this purpose, it deviates considerably from both the MODIS proxy model and the synthetic model. This is shown in Figure 1 for comparison.

4.2 *Modeling the Orbital Geometry*

An important part of the EVEREST simulation is the orbital geometry. The model computes the orbit of the satellite and solar azimuth and elevation angles along with the sensor azimuth and elevation angles for every point in the scene, and also the solar geometry with respect to VIIRS. It also computes lunar azimuth and elevation angles and the lunar phase for the nighttime scenes. Since solar and lunar illumination is highly correlated with the solar and lunar zenith angles respectively, it is important to consider what these values are at different parts of an orbit. It is also important to understand where in the orbit VIIRS switches from the day mode to the night mode, since the DNB calibration data can only be collected in the night mode. Figure 2 shows a simulation of the SZA as a function of latitude over 6 different points across a scan. The regions where the gain transfer calibration and the dark offset determination can be performed are also shown.

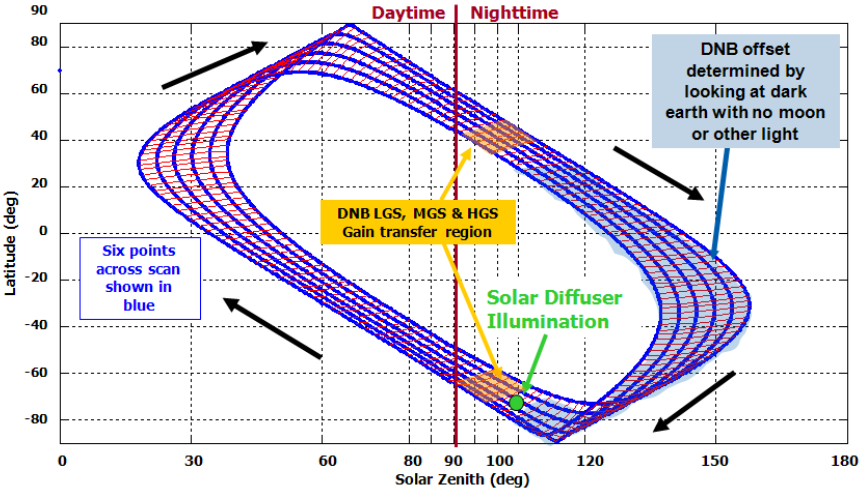

Figure 2 - SZA vs. Latitude for 1330 Orbit at Northern Summer Solstice

5. CALIBRATION PROCESS

On orbit the DNB will be calibrated with a simple linear approach. The calibration equation for the DNB radiance is

$$L = \mathrm{RVS}(n) \cdot A(m, N_{agg}(n), j) \cdot dn_{EV}(m,n,k)$$

with:

$$dn_{EV}(m,n,k) = DN_{EV}(m,n,k) - DN_{off}(m,n,j)$$

and where:

L = calibrated earth view radiance
RVS = Response vs. Scan angle
m = index for in-track detector #
n = index for cross-track pixel
k = index for scan number
j = index for gain stage (1 to 3)
A = gain converting counts to radiance
N_{agg} = aggregation zone, maps to n
DN_{EV} = observed earth view counts
DN_{off} = offset value for earth view
dn_{EV} = offset adjusted earth view counts

RVS is measured prelaunch and N_{agg} is known by design, so the purpose of the on-orbit calibration is determining the offset, DN_{off}, and the gain coefficient, A.

5.1 *Aggregation Zones*

In addition to 3 gain stages, another complication for calibration is the method the DNB uses to maintain a near constant 750 m resolution across its entire 3000 km swath. It achieves this by varying the aggregation of the individual pixels on its CCD. This requires 32 aggregation zones across the swath. Each zone aggregates a different number of individual CCD pixels in scan and in-track compensating for perspective and foreshortening. Therefore, the zones near the edge of the swath have the least number of pixels aggregated and the zone at nadir has the most. Because the aggregating is done on-board, ground calibration must calibrate each aggregation zone separately. The gains for the aggregation zones are nearly inversely proportional to the number of pixels aggregated, but not exactly enough to calibrate them as a whole.

5.2 *Calibration Sources*

The on-board reflective calibration source is a solar diffuser (SD), which is observed once per scan. A space view (SV) port is also used for an offset. Every 2 scans the DNB observes the calibration view with a different aggregation mode. Calibration view data for both the SV and the SD are reported by all gain stages. The SD is illuminated for about a minute once per orbit, and this data is accumulated, but since it takes 72 scans to cycle through the complete calibration cycle, this is not enough time to cycle through all the aggregation modes. Therefore, calibration must be collected over multiple orbits for the DNB.

The SD data is accumulated to calibrate the low-gain mode. Though the MGS and HGS data are collected, they become saturated when observing the sun illuminated SD, and so this cannot be used for calibration.

5.3 *Offset Determination*

The space view provides a zero radiance offset which is subtracted from the solar diffuser for LGS gain determination. However, the zero offset observed in the calibration views is slightly different from the zero offset observed in the earth view, and a more accurate method of determining DN_{off} requires the use of dark views from the earth view. The darkest scenes of the earth are during a new moon, and data is collected from all three gain stages to do this. In normal operating mode, only the HGS is transmitted at night. However, it is possible for separate DNB MGS and LGS earth view data, if specially commanded, to be transmitted only during night mode. Figure 3 shows simulated data for the 3 gain stages that would be collected over a dark earth scene. The vertical banding clearly shows the 32 aggregation zones (repeated twice and symmetric about nadir – approximately sample 2000) with a different offset for each. There is also clearly striping from detector to detector, and since these images represent 16 scans of data, there is a pattern of the striping repeated 16 times.

After the dark earth view data has been collected, it is geo-located and then needs further filtering. Obviously, populated areas will have enough light at night to bias the offset, at least for HGS. Therefore, regions with known human habitation are removed. A conservative approach is to eliminate all land, but our baseline threshold will be to use only regions with less than 4 persons per km^2 based on population density maps. A more conservative approach would be to eliminate all land areas.

Another possible light source is aurora activity. By eliminating data from north or south latitudes greater than 50 degrees almost all aurora activity will be suppressed.

Even with these filters there will be some night lights that pass the filtering (e.g. ships on the ocean, lightning or mid-latitude auroras).

To do further filtering data is binned by detector, m, in-scan pixel, n and gain stage,

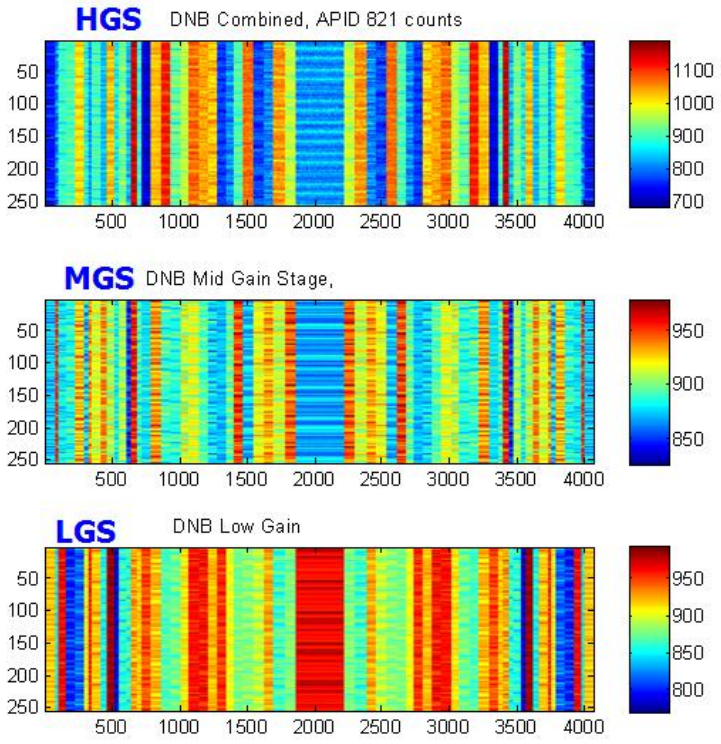

Figure 3- Simulated raw counts for 16 scans of dark earthview data for LGS, MGS and HGS

j. Once enough data is collected, statistics are taken determining mean, standard deviation, skew and kurtosis. The skew and kurtosis are used to determine whether there are any pixels included in the bin which are not totally dark. The skew and kurtosis of the distribution is taken, and if a bin has values of skew and kurtosis well beyond what is expected for a normal distribution, then outliers are identified and removed and the average value of the offset is retaken.

5.4 *Gain for LGS*

The calibration of the LGS uses the SD view and is similar to the process used for the other VIIRS reflective bands, which has been described elsewhere (DeLuccia 2009; Mills 2007). LGS is the only stage able to use the SD directly for calibration because MGS and HGS saturate when the SD is illuminated. In short, the LGS calibration process compares expected radiance on the solar diffuser based on the solar geometry with the counts from solar diffuser with space view (SV) subtracted. This yields a value for gain, but unlike the other bands, the DNB requires each of the 32 aggregation zones to be calibrated separately. The gain is computed as follows:

$$A(m, N_{agg}, 1) = \frac{L_{sd}(\vec{\theta}, d_{se})}{dn_{SD}(m, N_{agg}, 1)}$$

where:

$$dn_{SD}(m, N_{agg}, 1) = DN_{SD}(m, N_{agg}, 1) - DN_{SV}(m, N_{agg}, 1)$$

and

$$L_{sd}(\vec{\theta}, d_{se}) = \mathrm{RVS}_{sd} \cdot \pi \cdot \overline{E}_{sol} \cdot \cos(\theta_{inc}) \cdot \rho(\vec{\theta}) \cdot \tau(\vec{\theta}) \cdot \left(\frac{\overline{d_{se}}}{d_{se}} \right)^2$$

with:

L_{sd} = computed radiance of SD
RVS_{sd} = RVS at the SD scan angle
DN_{SD} = scan averaged SD counts
DN_{SV} = scan averaged SV counts
dn_{SD} = scan averaged, offset adjusted SD counts
ρ = index for scan number
τ = index for scan number
$\vec{\theta}$ = 2-dimensional angle of the sun relative to the sensor
θ_{inc} = angle of incidence of the sun on the SD; is a function of $\vec{\theta}$
d_{se} = sun-to-earth distance
$\overline{d_{se}}$ = annually averaged sun-to-earth distance
$\overline{E}_{sol}$ = annually averaged solar spectral irradiance

5.4 *Gain Transfer for MGS & HGS*

Since MGS and HGS saturate when the SD is illuminated, calibration is accomplished indirectly using the Earth view data in the transition regions between the stages. VIIRS has the capability of transmitting the gain stage data separately, and to perform cross-calibration between the stages, separate data from all 3 stages must be transmitted.

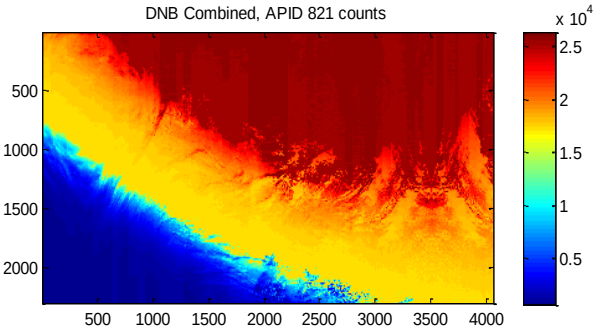

Figure 4 - Simulated DNB earth view scene data modeled from EVEREST over a 1700 km by 3000 km region crossing the terminator.

Figure 4 shows simulated DNB scene with dn_{EV} computed from EVEREST. It is in a region crossing the terminator, where radiances span 6 orders of magnitude. This span of radiance covers all 3 gain stages as is shown in Figure 5. There is a limited region where the low-gain is sensitive but the MGS is not saturated, and the calibration process identifies these regions and then takes the ratios of the data to determinate a

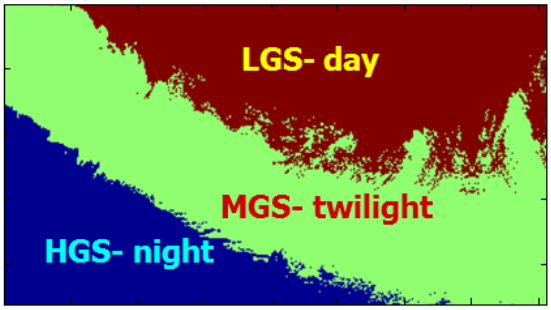

Figure 5 - Gain stages selected by DNB in normal operating for radiances in Figure 4.

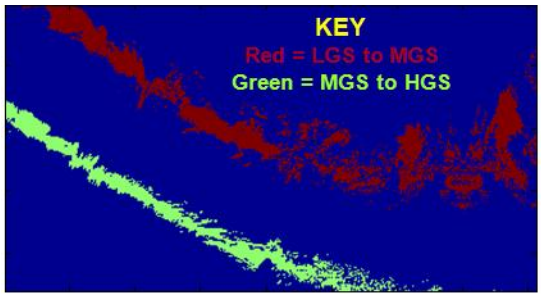

Figure 6 - Transition region used to determine MGS/LGS gain ratio (red) and HGS/MGS gain ratio (green).

relative gain. In this crossover region the LGS Signal-to-Noise Ratio (SNR) is low, and the lower threshold is determined by where the SNR drops below an acceptible level, which is initially set to 25, but can be tuned. A similar process is done to determine the crossover region between MGS and HGS. In Figure 6 these two regions are shown for the scene in Figure 4.

Once the LGS to MGS gain transition region is identified, the ratio of dn_{EV} from the LGS is computed for each pixel, and the ratios are binned by detector number, m, and aggregation zone, N_{agg}, and when the number of points in each bin exceeds a threshold (>1000 is reasonable) the ratios in each bin are averaged, and the gain for MGS is computed using the equation

$$A(m, N_{agg}, 2) = \overline{R_{M:L}}(m, N_{agg}) \cdot A(m, N_{agg}, 1)$$

$$\text{where } \overline{R_{M:L}} = \text{averaged MGS : LGS } dn_{EV} \text{ ratio}$$

A similar process is used to compute the HGS gain with the equation

$$A(m, N_{agg}, 3) = \overline{R_{H:M}}(m, N_{agg}) \cdot A(m, N_{agg}, 2)$$

$$\text{where } \overline{R_{H:M}} = \text{averaged HGS : MGS } dn_{EV} \text{ ratio}$$

6. STRAY LIGHT MODEL & FLAGGING

Because of the DNB, VIIRS was designed to minimize stray light. Nevertheless there are rare conditions where stray light is strong enough to have a noticeable impact on imagery. This impact is increasing the background level in a scene and, consequently, reducing contrast.

The most challenging stray light conditions occur where there are large contrasts, and this occurs most particularly around the terminator when both day and night are seen in close proximity. Figure 7 shows the geometry of the earth view as seen by VIIRS for a terminator crossing.

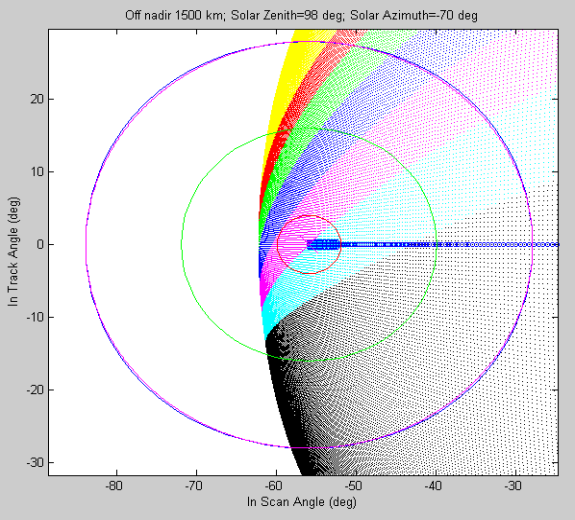

Figure 7 - Geometry of the sun side of the scan near the edge of scan when crossing near the terminator. Red, green & purple circles indicates 5, 15 and 30 deg off optical axis respectively. The colored bands indicate SZA regions from 88 to 100 deg.

The points on the surface of the Earth are equally spaced and this produces an image of the curvature of the Earth. Note that as the surface drops off toward the horizon the SZA regions are compressed from foreshortening. The blue vertical line shows a VIIRS scan and the circles are centered at the edge-of-scan. Note the green circle that encompasses the area within 15º of that point. The circle extends out to the yellow region which indicates area where the SZA < 90º, where the earth is lit by the sun. From Figure 1 it is seen that the 15º region spans 5 orders of magnitude of radiance. Stray light rapidly drops off from the boresite, but under these extreme scene conditions there is enough stray light to have an effect.

Modeling has been done to determine the extent of stray light over a typical orbit, and is shown in Figure 8. The plot shows the ratio of expected stray light to average scene radiance, and peak up to 3% is seen. For 1% of all scenes over an orbit, stray light

is significant. The impact is to cause a somewhat lower contrast image, but the

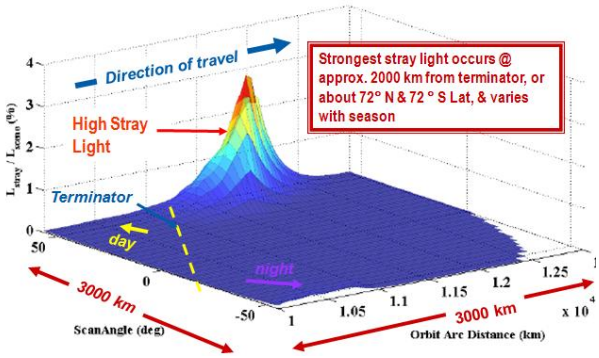

image is still useful. Rather than try to calibrate the impact of stray light, the calibration algorithm identifies and flags the limited cases of high stray light.

Figure 8 - Modeled DNB stray light. Ratio of expected stray light to average scene radiance. A peak up to 3% is seen.

7. CONCLUSIONS

The zero radiance offset is determined using the earth view of a moonless scene. A methodology for gain calibration of the DNB LGS from the Solar Diffuser has been described. Transfer of gain calibration from LGS to MGS uses specially transmitted LGS & MGS data in a very limited overlap region to determine a gain ratio.

Similarly, transfer of gain calibration from MGS to HGS uses specially transmitted MGS data and the HGS data from the normal earth view in a very limited overlap region to determine a gain ratio.

Stray light has been modeled, and has been determined to be small except for a small region near the terminator that is < 1% of all scenes.

REFERENCES

Akasofu, S. I., 1974: A study of auroral displays photographed from the DMSP-2 satellite and from the Alaska meridian chain of stations. *Space Science Reviews,* **16**, 617-725.

Croft, T. A., 1978: Night-time images of the earth from space. *Sci. Amer.,* **239,** 86–98.

De Luccia, F., E. Johnson, S. Mills, X. Xiong, B. Guenther, J. McCarthy, D. Moyer and M. Bliton, 2009: NPP Visible/Infrared Imaging Radiometer Suite (VIIRS) Radiometric Calibration and Predicted Data Product Performance. *2009 IEEE International Geoscience and Remote Sensing Symposium (IGARSS)*, MO4.O9.2.

Elvidge, C. D., H. W. Kroehl, E. A. Kihn, K. E. Baugh, E. R. Davis, and W. M. Hao, 1996: Algorithm for the retrieval of fire pixels from DMSP Operational Linescan System Data. *Biomass Burning and Global Change: Remote Sensing, Modeling and Inventory Development, and Biomass Burning in Africa,* J. S. Levine, Ed., MIT Press, 73–85.

——, K. E. Baugh, E. A. Kihn, H. W. Kroehl, and E. R. Davis, 1997: Mapping of city lights using DMSP Operational Linescan System data. *Photogramm. Eng. Remote Sens.,* **63,** 727–734.

——, K. E. Baugh, V. R. Hobson, E. A. Kihn, and H. W. Kroehl, 1998: Detection of fires and power outages using DMSP-OLS data. *Remote Sensing Change Detection: Environmental Monitoring Methods and Applications,* R. S. Lunetta and C. D. Elvidge, Eds., Ann Arbor Press, 123–135.

Foster, J. L., 1983: Night-time observations of snow using visible imagery. *Int. J. Remote Sens.,* **4,** 785–791.

——, and D. K. Hall, 1991: Observations of snow and ice features during the polar winter using moonlight as a source of illumination. *Remote Sens. Environ.,* **37,** 77–88.

Hutchison, K. D., J. K. Roskovensky, J. M. Jackson, A. K. Heidinger, T. J. Kopp, M. J. Pavolonis, R. Frey, 2005: Automated cloud detection and classification of data collected by the Visible Infrared Imager Radiometer Suite (VIIRS), . *Int. J. Remote Sens.,* **26**, 4681 – 4706.

Jacobson, E., A. Ibara, M. Lucas, R. Menzel, H. Murphey, F. Yin, and K. Yokoyama, 2010: Operation and Characterization of the Day/Night Band (DNB) for the NPP Visible/Infrared Imager Radiometer Suite (VIIRS), *Am. Met. Soc., 6th Annual Symposium on Future National Operational Environmental Satellite Systems-NPOESS and GOES-R*, 349.

Lee, T. E., S. D. Miller, F. J. Turk, C. Schueler, R. Julian, S. Deyo, P. Dills, and S. Wang , 2006: The NPOESS VIIRS Day/Night Visible Sensor. *Bull. Am. Met. Soc.,* Feb. 2006, 191–199

Miller, S. D., T. F. Lee, F. J. Turk, A. P. Kuciauskas and J. D. Hawkins, 2005: Shedding new light on nocturnal monitoring of the environment with the VIIRS day/night band. *SPIE Proc.*, **5890,** 58900W1–58900W-9.

——, S. H. D. Haddock, C. D. Elvidge and T. F. Lee, 2006: Twenty thousand leagues over the seas: the first satellite perspective on bioluminescent "milky seas", *Int. J. Remote Sens.* 27, 5129.

Mills, S., 2004: Simulation of Earth Science Remote Sensors with NGST's EVEREST/VIRRISM. *AIAA Space 2004 Conf. Proc.,* **5954**

—— and J. Lamoureux, 2008: Simulation and test of the VIIRS Sensor Data Record (SDR) algorithm for NPOESS Preparatory Project (NPP). *AMS 87th Annual Meeting, NPOESS/GOES-R Symposium*, P2.8

Orville, R. E., 1981: Global distribution of midnight lightning—September to November 1977. *Mon. Wea. Rev.,* **109,** 391–395.

——, and R. W. Henderson, 1986: Global distribution of midnight lightning: September 1977 to August 1978. *Mon. Wea. Rev.,* **114,** 2640–2653.

Shoucri, M., B. Hauss, 2009: EVEREST: an end-to-end simulation for assessing the performance of weather data products produced by environmental satellite systems. *SPIE Proc.*, **7458**, 74580G-74580G-9.